Science of the Total Environment 859 (2023) 160189

Contents lists available at ScienceDirect

Science of the Total Environment

journal homepage: www.elsevier.com/locate/scitotenv

A palynological record of mangrove biogeography, coastal geomorphological change, and prehistoric human activities from Cedar Keys, Florida, U.S.A.

Qiang Yao [a], Kam-biu Liu [b], Erika Rodrigues [a,c], Daidu Fan [d], Marcelo Cohen [a,e,*]

[a] Department of Oceanography and Coastal Sciences, Louisiana State University, Baton Rouge, LA 70803, United States of America
[b] Department of Oceanography and Coastal Sciences and Coastal Studies Institute, Louisiana State University, Baton Rouge, LA 70803, United States of America
[c] Institute of Geosciences, University of São Paulo, São Paulo, Brazil
[d] School of Ocean and Earth Science, Tongji University, 1239 Siping Road, Shanghai 200092, China
[e] Graduate Program of Geology and Geochemistry, Federal University of Pará, Av. Perimentral 2651, Terra Firme, 66077-530 Belém, PA, Brazil

HIGHLIGHTS

- Temperature is the primary factor regulating mangrove distribution at the higher latitudes.
- Local factors regulate mangrove dynamics at the lower latitudes.
- Poleward mangrove migration in North and South America were synchronized during the last millennium.
- MCA likely facilitated poleward mangrove migration in North and South America
- A Woodland Native community settled on Seahorse Key prior to 500 cal yr BP.

GRAPHICAL ABSTRACT

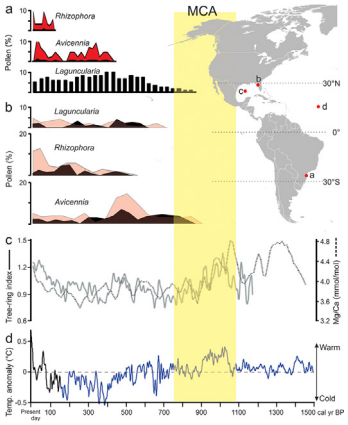

ARTICLE INFO

Editor: Manuel Esteban Lucas-Borja

Keywords:
Mangrove
Medieval climate anomaly
Palynology
Woodland native culture
Cedar keys
Gulf of Mexico

ABSTRACT

Under the continuous warming trend in the 21st century, mangroves are likely to migrate into more temperate regions in North and South America. However, the biogeography of different mangrove species is still unclear, especially near their latitudinal range limits in the two continents. This study utilizes palynological, geochemical, and sedimentological analyses to record changes in the coastal morphology and vegetation during the Holocene in Cedar Keys, Florida, the mangrove sub-range limit in North America. The multi-proxy dataset indicates that the milder winters during the Medieval Climate Anomaly likely facilitated the establishment of mangroves in the study region, where *Avicennia*, *Laguncularia*, and *Rhizophora* were established in the ~12th (790–850 cal yr BP), ~14th (580–660 cal yr BP), and ~ 16th century (440–460 cal yr BP), respectively. Thus, the Medieval Climate Anomaly likely triggered the poleward mangrove migration in North and South America synchronously. Moreover, the multi-proxy dataset also documents the obliteration of the Woodland Culture near Cedar Keys, where a once-thriving native civilization on Seahorse Key was driven out by the European colonizers, who settled on the mainland and Atsena Otie Key. Over time, the relict sites of the Woodland people on Seahorse Key were covered by mangroves and marsh vegetation since the ~16th century. Overall, our dataset suggests that industrial-era warming may have intensified the poleward mangrove expansion, although this trend had started earlier during the Medieval Climate Anomaly.

* Corresponding author at: College of the Coast & Environment, Louisiana State University, 93 South Quad Drive, United States of America.
E-mail address: mcohen@ufpa.br (M. Cohen).

http://dx.doi.org/10.1016/j.scitotenv.2022.160189
Received 29 August 2022; Received in revised form 9 November 2022; Accepted 10 November 2022
Available online 14 November 2022

1. Introduction

In the face of accelerating global warming, poleward migration of mangroves is documented worldwide (Ellison, 2002; Gilman et al., 2008; Walker et al., 2019; Osland et al., 2021). In North America, mangroves have been expanding into salt marshes along the Gulf of Mexico (GOM) and Atlantic coasts during the past 30 years (Cavanaugh et al., 2014, 2019; Osland et al., 2017, 2022; Yao et al., 2022a, 2022b). The two coastal plant communities support unique fauna and flora and provide many important socio-ecological services (Barbier et al., 2011), such as carbon sequestration (Kauffman et al., 2011), organic matter exportation (Dittmar et al., 2006), shoreline protection against coastal hazards (Hutchison et al., 2014), and pollution control (Barbier et al., 2011). Thus, mangrove invasion into salt marsh habitats is becoming a focus of research and concern for ecologists and stakeholders in North America.

Rhizophora mangle (red mangrove), *Avicennia germinans* (black mangrove), and *Laguncularia racemosa* (white mangrove) are the only three true mangrove species found in North America, with *Avicennia germinans* being the most cold-tolerant species among the three (Tomlinson, 2016). During the last glacial maximum (~21,000 years BP), the range of North American mangroves was limited to Central America (Sherrod and McMillan, 1985). After the last deglaciation, due to the warming climate (Clark et al., 2009), mangroves started to expand and migrate toward higher latitudes during the Holocene (Woodroffe and Grindrod, 1991; Kennedy et al., 2016), and eventually established in the continental United States in South Florida ~4000 cal yr BP (Yao and Liu, 2017; Jones et al., 2019). The modern global distribution of mangroves is greatly influenced by extreme freeze events (Stevens et al., 2006; Quisthoudt et al., 2012; Alongi, 2015; Osland et al., 2019, 2020). Winter freezes (< −4 °C) cause defoliation or mortality to *Avicennia germinans* (Ross et al., 2009), hence limiting its migration toward high latitudes (Stuart et al., 2007; Osland et al., 2013). Historically, the boreal mangrove range limit in the continental United States was located in Cedar Keys, Florida, at ~29°N (Little, 1978). However, with the increasingly warm winters during the past few decades, poleward mangrove migration accelerated in the 21st century (Yao et al., 2022b) (Fig. 1), while more and more *Avicennia germinans* colonies have been spotted along the northern GOM coasts (~30°N) in the Florida Panhandle (Snyder et al., 2022; Yao et al., 2022a), Louisiana (Cohen et al., 2021; Rodrigues et al., 2021; Ryu et al., 2022), and Texas (Montagna et al., 2011; Osland et al., 2013). Thus, the biogeography of *Avicennia germinans* in the continental United States exhibited a gradual poleward migration following the temperature gradient, as with other species in Florida (Box et al., 1993).However, most studies regarding mangrove tropicalization in North America were focused on *Avicennia germinans* due to its greater tolerance to low winter temperatures (Armitage et al., 2015; Cook-Patton et al., 2015; Osland et al., 2020), while very few studies have documented the long-term dynamics of *Rhizophora mangle* and *Laguncularia racemosa* during the Holocene (Cavanaugh et al., 2014, 2019; Yao et al., 2022a, 2022b), especially from their sub-range limit. We define mangrove sub-range limit (~26°–29°N) as areas proximate to their poleward range limit (~30°N), where all three mangrove species can proliferate. These areas are key to unlocking the biogeographic history of all three mangrove species, because the climate anomalies exert greater influence on all three mangrove species across these latitudes, especially during the Medieval Climate Anomaly (MCA, ~1050 to 750 cal yr BP), when the northern GOM sea surface temperature was supposedly warmer than the present-day (Richey et al., 2007). Hence, it is still unclear whether the mangrove migration toward the northern GOM corresponded to the late Holocene climate variability or was solely an Anthropocene (post-1950s) phenomenon.

Moreover, recent studies from South America indicate that poleward mangrove migration was mainly controlled by temperature and the availability of muddy substrate, which is the preferred sedimentary environment for mangrove establishment (França et al., 2019; Bozi et al., 2021; Figueiredo et al., 2021). *Laguncularia racemosa* established first in the mangrove sub-range limit near São Francisco do Sul Bay, Brazil (~26°N) at ~900 cal yr BP (Rodrigues et al., 2022), and it took ~900 years for *Avicennia germinans* and *Laguncularia racemosa* to reach their current austral range limit near southern Santa Catarina, Brazil (~28°N) (Cohen et al., 2020a). In this context, it is still unclear whether the expansion of different mangrove species followed

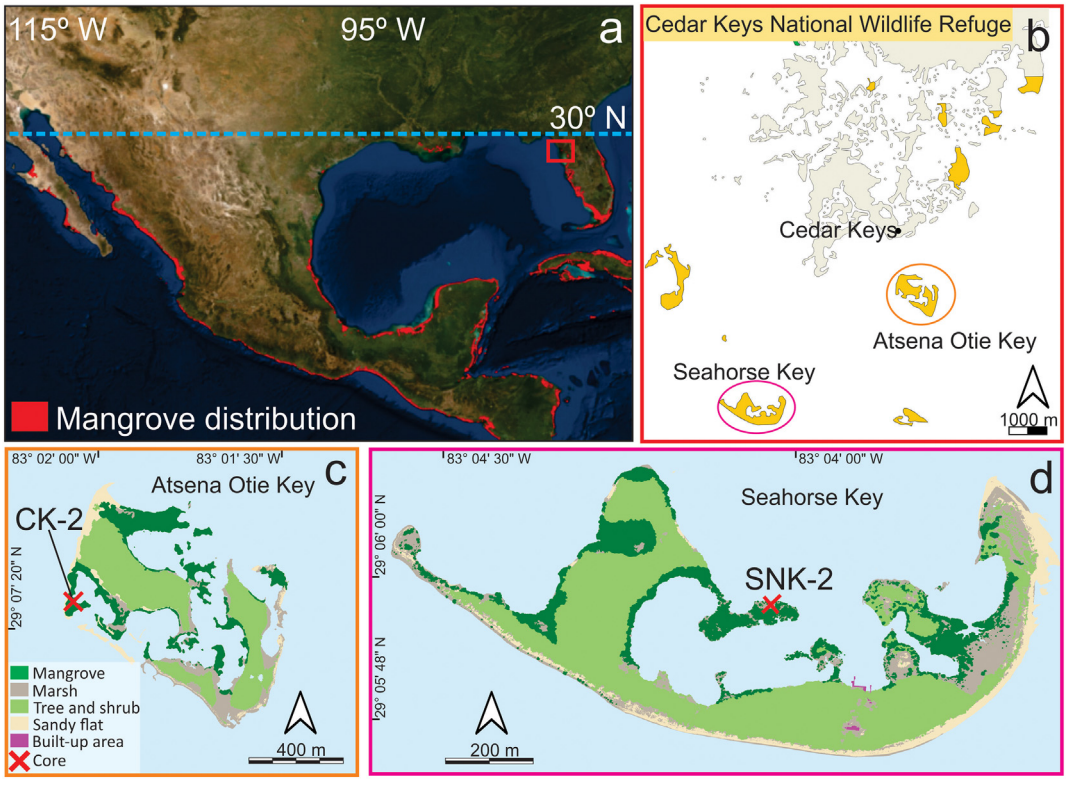

Fig. 1. (a) Mangrove distribution in North America; red rectangle marks the study area; (b) Map of Cedar Keys National Wildlife Refuge; morphological and vegetation features of the two coring sites on (c) Atsena Otie Key and (d) Seahorse Key. The red crosses in (c) & (d) mark the location of core CK-2 and SNK-2, respectively.

the same temperature gradient in North America. In particular, is poleward mangrove migration synchronized in both North and South America throughout the Holocene? This information is vital for predicting the global distribution of different mangrove species and associated ecological responses under the rapid climate change in the 21st century. Thus, large data gaps exist in the literature.

Cedar Keys, Florida is 200 km to the southeast of the current boreal mangrove range limit and home for all three mangrove species in North America (Little, 1978). Thus, this mangrove sub-range limit site is a critical location to investigate the biogeography of the three mangrove species. In this paper, we utilize palynology, grain-size, loss-on-ignition (LOI), and X-ray Fluorescence (XRF) on two sediment cores (CK-2 and SNK-2) to reconstruct the late Holocene mangrove biogeography and coastal morphological change in the Cedar Keys National Wildlife Refuge (Fig. 1). The overarching objectives of this study are to answer these three research questions: 1) Is mangrove expansion in North America associated with any climate anomalies during the late Holocene? 2) Is poleward mangrove migration in North America synchronized with that in South America during the Holocene? 3) What drives different mangrove species to migrate from South Florida toward the northern GOM? In addition, our cores contain a thick shell layer likely representing a shell midden attributed to the Woodland Native Culture. Thus, this study also documents the prehistoric human activities in the study region.

2. Materials and methods

2.1. Geographic background of the study area

Cedar Keys National Wildlife Refuge (~29°10′ to 29°5′ N, ~83°5′ to 82°6′ W) is comprised of 13 islands (highlighted in yellow color in Fig. 1b) ranging from 0.4 to 50 ha in size. Most of the islands sit on the Seahorse Reef, a ridge of shallow bottom (0.5–1 m) that lies due south of the town of Cedar Keys (https://www.fws.gov/refuge/cedar-keys). The climate of this region is humid subtropical, but the Atlantic hurricane season strongly influences the rainfall pattern (Biasutti et al., 2012). The average annual precipitation (U.S Climate Data, n.d.), winter daily minimum air temperature, and relative sea-level (RSL) rise trend at Cedar Keys are ~1500 mm, ~11 °C, and 2.3 mm/yr, respectively (NOAA CO-OPS, n.d.). Vegetation in the refuge is dominated by a combination of mangrove forest (containing all three mangrove species), maritime forest (pine and oak), and herbaceous plants such as graminoids, Amaranthaceae, and *Typha* (Field, 1991). Historically, Cedar Keys were regarded as the northern limit of continuous *Rhizophora mangle* and *Laguncularia racemosa* distribution on the Gulf Coast of Florida (Little, 1978). However, over the past few decades, mature *Avicennia germinans* colonies and sparse stands of *Rhizophora mangle* have been established in the Apalachicola area (~200 km northwest to Cedar Keys) along the Florida Panhandle (Snyder et al., 2022; Yao et al., 2022b).

In this study, we sampled Atsena Otie Key (~33,750 ha) and Seahorse Key (~36,411 ha), two of the largest islands in the refuge. Both islands are sitting on very shallow (~0.5 m) clam and oyster reefs, fringed by mangrove forests, while pine, oak and other shrubs occupy the island interiors (Fig. 1c&d). On Atsena Otie Key, *Avicennia germinans* (up to 5 m tall) dominates the mangrove forest but some *Rhizophora mangle* (<2 m) and *Laguncularia racemosa* trees (<2 m) are present. On Seahorse Key, the north side of the island is fringed by mixed mangrove forests containing all three species. *Laguncularia racemosa* (up to 2 m) grows inland from *Avicennia germinans* (up to 7 m), which themselves grow inland from *Rhizophora mangle* (up to 2 m). The pore water salinity on the two islands was 20 to 25 ‰ whenmeasured during the two field expeditions in December 2018 and 2019.

2.2. Field work and remotely-sensed data collection

Cores CK-2 (180 cm; from Atsena Otie Key, 29°7′23.60″ N, 83° 2′2.60″ W) and SNK-2 (195 cm; from Seahorse Key, 29°5′57.96″ N, 83°4′2.22″ W) were retrieved in December 2018 by means of a vibra-corer from the fringing mangrove forests on these two islands (Fig. 1c&d). Both cores were pushed in until refusal to capture the most complete depositional history possible. To identify the morphological and vegetation features of the study sites, drone surveys using a Phantom 4 Advanced DJI (spatial resolution of 1.6 cm/pixel at 60 m) with ground validation were conducted on each island during the field expeditions. Drone images were processed using Agisoft Metashape Professional version 1.6.2 and Global Mapper 22.1 to create the digital elevation models and identify vegetation units on the two islands, following the methodology described in Cohen et al. (2020b) and Yao et al. (2022c).

2.3. Laboratory analyses

Grain-size analysis was performed on both cores at 5-cm interval using a Beckman Coulter particle size analyzer (0.04–2000 μm range), following standard procedures described in Zhang et al. (2021). The distribution of sand (2–0.0625 mm), silt (62.5–3.9 μm), and clay fraction (3.9–0.12 μm) was determined following the methods developed by Wentworth (1922). Stratigraphy was described based on the color, lithology, and texture of the sediment types (Miall, 1978).

X-ray fluorescence (XRF) and loss-on-ignition (LOI) analyses were performed on both cores at 1-cm interval to measure the elemental concentration (ppm) of major elements and the % wet weight for water and % dry weight for organics and carbonates throughout the cores, following the standard laboratory procedures describe in Yao et al. (2020a, 2020b). For XRF analysis, five major chemical elements (Ca, Sr, Zr, Ti, and Fe as part per million - PPM) and Ca/Ti and Cl/Br ratios exhibited meaningful variations and were reported in this study.

A total of 58 samples consisting of ~1 cm^3 of sediment each were taken from core CK-2 and SNK-2 at 5-cm interval for palynological analysis. All samples were processed following the standard procedure described in Yao and Liu (2018). One *Lycopodium* tablet (~20,848 grains) was added to each sample as an exotic marker to calculate the pollen concentration (grains/cm^3). A minimum of 300 pollen grains were counted for each sample (except for samples from 130 to 190 cm in core SNK-2 where the pollen concentration is very low) to ensure the results were statistically robust. In addition, foraminifera linings, dinoflagellate tests, and charcoal fragments (>10 μm in size) were also counted. Due to the overwhelming amount of *Pinus* pollen throughout both cores, they were excluded from the calculation of pollen percentages. Published pollen keys (Willard et al., 2004; Yao and Liu, 2018) were used as references to identify the palynomorphs. TILIA and TILIAGRAPH software were used for calculation and plotting the pollen diagram (Grimm and Troostheide, 1994). CONISS was used for cluster analysis of the pollen taxa (Grimm, 1987). Based on extensive pollen surveys from mangrove forests across the North and South America (Yao et al., 2015, 2021, 2022a, 2022b; Cohen et al., 2020a, 2020b, 2021), the continuous appearance of mangrove pollen (>2 %) is used as a threshold to identify the establishment of mangrove forest. A step-by-step preparation procedure of pollen samples and an atlas and identification key of the common pollen types from the study region are listed in the co-submitted MethodsX (Yao et al., in review a) and Data-in-Brief articles (Yao et al., in review b).

2.4. Radioisotopic dating

Six samples consisting of bulk organic sediments were sent to ICA Inc., in Florida, for AMS ^{14}C dating (Table 1). All ^{14}C samples were pretreated to eliminate fibrous roots and shell fragments, following the methodology described in Yao et al. (2022d). Twenty-five samples from the top 75 cm in core CK-2 were sent to the State Key Laboratory of Marine Geology, Tongji University, China for ^{210}Pb and ^{137}Cs dating at 3-cm interval. Gamma-ray measurements were performed on a HPGe well type γ-ray detector (GWL-120-15-LB-AWT, AMETEK). Excess ^{210}Pb ($^{210}Pb_{ex}$) activity was determined by subtracting the supported ^{210}Pb ($^{210}Pb_{su}$, equivalent to 226Ra) from total ^{210}Pb ($^{210}Pb_t$). The surface sediment intervals (0–5 cm) were scanned in the detector for 48 h. The Constant Initial

Table 1
Radiocarbon dating results for core CK-2 and SNK-2.

Core ID	Depth (cm)	Age (^{14}C yr BP)	Calibrated range (cal yr BP, 2σ deviation)	Weighted mean (cal yr BP)
CK-2	40	0 ± 20	−26–270	150
CK-2	70	580 ± 40	480–660	580
CK-2	150	1510 ± 40	1280–1540	1410
SNK-2	50	280 ± 30	120–450	350
SNK-2	95	1340 ± 30	1080–1380	1260
SNK-2	150	4020 ± 40	3870–4680	4410

Concentration (CIC) model was applied to calculate the sedimentation rate (Goldberg, 1963; Robbins and Edgington, 1975). Fitting analysis was done using the 'Exp2PMod1' function in Origin 2018 program. The ^{14}C and short-lived isotope dating results were imported into *RBACON version 2.2* to generate an age-depth model (Blaauw and Christen, 2011). All dates were converted to calibrated years before present (cal yr BP) and rounded to the nearest decade, using 1950 CE as 0 cal yr BP.

3. Results

3.1. Chronology model

For short-lived isotopic dating, a ^{137}Cs peak is detected at 25 cm in core CK-2 (Fig. 2), marking the maximum nuclear fallout at 1963 CE, and a vertical accretion rate of 4.54 mm/yr (0–25 cm) is inferred assuming a constant accretion rate. The depth profile of $^{210}Pb_{ex}$ shows a relatively steady exponential decay trend for the top 50 cm in core CK-2. According to the CIC model, it reveals a sedimentation rate of 6.5 mm/yr (constant = 0.0311; Corbett and Walsh, 2015).

All ^{14}C dates were deemed valid by the Bayesian model (Fig. 3). Bayesian statistical methods have been used to perform interpolation and construct uncertainty estimates that account for possible sedimentation rate changes throughout the cores (Lisiecki et al., 2022). Based on *RBACON*, the calibrated radiocarbon dates ranged from ~4410 to 0 cal yr BP (Table 1). Collectively, we used the weighted mean age (the red curve in Fig. 3) estimated by *RBACON* to construct the chronologies for the two cores. The Bayesian model revealed a relatively consistent sedimentation rate for core CK-2, with a basal age of ~1700 cal yr BP (Fig. 3a). Core SNK-2 has a basal age of ~6700 cal yr BP and a relatively constant sedimentation rate down to 95 cm from the top, below which the sedimentation rate decreased by four-folds (Fig. 3b). The calibrated range and weighted mean age given by the Bayesian model for each depth interval in both cores are listed in the Supplementary Content (Table S1).

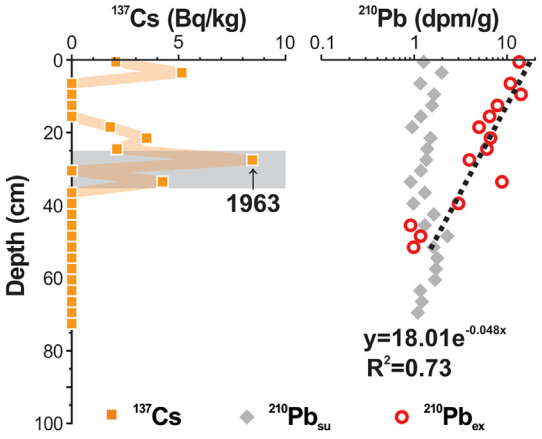

Fig. 2. ^{137}Cs (left) and ^{210}Pb (right) dating results of core CK-2.

3.2. Stratigraphic, sedimentary, and geochemical datasets

Visual inspection and multi-proxy analyses revealed that core CK-2 consists of three different types of sediments (Fig. 3a), including fine-sand (180–115 cm), coarse-sand (115–75 cm), and muddy-sand (75–0 cm). Sediments in the fine-sand section are characterized by abundant shells of *Crassostrea virginica* (oyster) and *Anadara* sp. (clam), very low water, organic, and carbonate content, and relatively high values of marine elements (Ca, Sr, Zr) and Cl/Br ratio (Fig. 4a)—the latter is a normalized parameter associated with salinity (Liu et al., 2014; Yao et al., 2020a). The coarse-sand section exhibits similar sedimentological and geochemical characteristics as the fine-sand section, except for coarser grain-size, hence the content of Zr – the main constituent for Florida beach sand (Miller, 1945) – is also the highest throughout the core. The top 75 cm of core CK-2 (muddy-sand section) is characterized by relatively finer grain-size, substantially higher contents of water, organics, and carbonates, and decreasing Cl/Br ratio (Fig. 4a).

Core SNK-2 also consists of three types of sediments, including sandy-silt (195–100 cm), silt (100–65 cm), and muddy-sand (65–0 cm) (Fig. 3b). The sedimentological and geochemical characteristics of the sandy-silt section highly resemble those of the bottom fine-sand section in core CK-2, except for the assortment of shells. In core SNK-2, intact shells of *Anadara* sp. and some small oysters (195–160 cm) underlie big intact oyster shells (160–130 cm), which themselves underlie broken oyster hash (130–100 cm) (Fig. 3b). Accordingly, the oyster hash section (130–100 cm) is characterized by the highest values of carbonates, Ca, Sr, and Ca/Ti, typical indicators for marine sediments and shells (Ramírez-Herrera et al., 2012; Yao and Liu, 2018; Williams et al., 2022), between both cores (Fig. 3b). Above the shell beds, the silt section is characterized by much smaller grain-size, increased water and organic contents, and a higher value of Fe, a typical indicator for terrestrial runoff (Haug et al., 2001; You, 2008; van Soelen et al., 2012). At the top 65 cm in core SNK-2, the sedimentological and geochemical characteristics of the muddy-sand section highly resemble those of the muddy-sand section at the top of core CK-2 (Fig. 4b).

3.3. Pollen data

A total of 36 pollen and spore taxa were identified from core CK-2, but only palynomorphs occurring at >2 % in any interval are plotted (Fig. 5). Core CK-2 is divided into three pollen zones, based on the stratigraphy and CONISS analysis. The pollen assemblage in Zone-A (180–130 cm, 1700–1200 cal yr BP) is dominated by upland (~40 %) and marsh (~60 %) taxa (Figs. 4 and 5). Specifically, most pollen spectra in Zone-A contain abundant *Quercus* (Oak) and Amaranthaceae (>40 %), indicating a freshwater and brackish marsh commonly found along the Florida Gulf coastlines (Willard et al., 2004; Yao et al., 2015). Mangrove pollen made its first appearance in Zone-B (130–75 cm, 1200–640 cal yr BP) (Figs. 4 and 5), characterized by a single *Avicennia germinans* grain at 130 cm and abundant *Avicennia germinans* pollen (~3 %) above 90 cm (790 cal yr BP). Apart from this, *Quercus* and Amaranthaceae are still the most abundant pollen taxa, while the concentrations of foraminifera and dinoflagellate increased substantially in this zone (Fig. 5). Pollen concentrations (including *Pinus*) increased significantly in Zone-C (75–0 cm, 640 cal yr BP to present) (Figs. 4 and 5), and pollen grains of *Laguncularia racemosa* and *Rhizophora mangle* start to occur continuously above 70 (580 cal yr BP) and 60 cm (440 cal yr BP), respectively (Fig. 5). In addition, concentrations of foraminifera linings, dinoflagellate tests, and charcoal fragments increase substantially throughout Zone-C, while pollen of Cyperaceae, Asteraceae, and other graminoids (e.g., Poaceae >40 μm) also become more abundant.

A total of 30 pollen and spore taxa are identified from core SNK-2, divided into 4 zones (Figs. 4 and 6). Zone-NP (195–130 cm, 6700–3200 cal yr BP) contains plentiful foraminifera linings and dinoflagellate tests but too few (<50 grains in each sample) pollen and other non-pollen palynomorphs to show a meaningful statistical relationship, hence, it is marked as "Pollen poor" (Fig. 6). Above this barren section, tree, shrub, and marsh taxa start

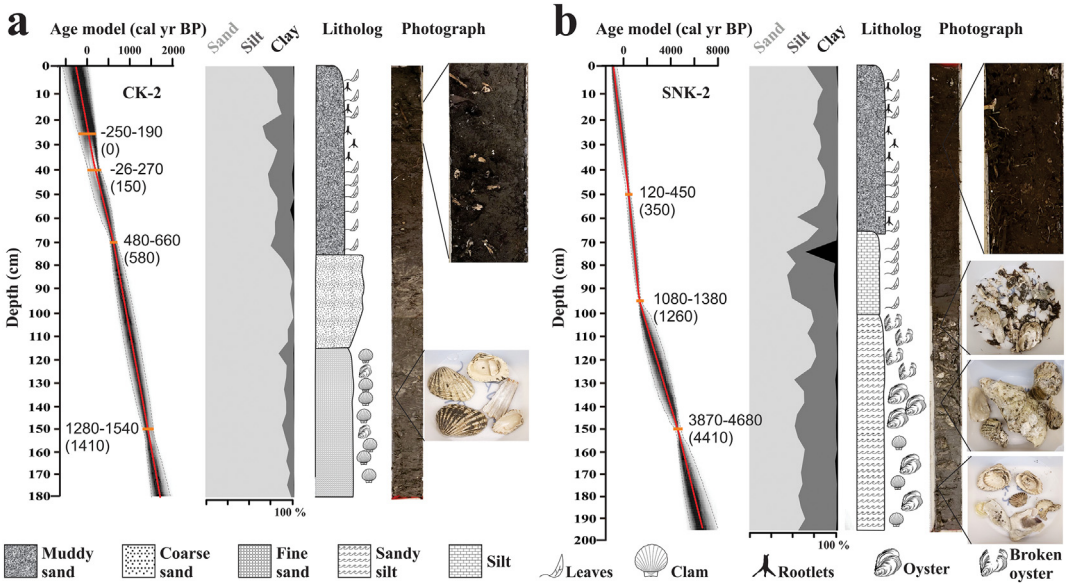

Fig. 3. From left to right: the Bayesian age-depth model, grain-size result, litholog, and photographs for core (a) CK-2 and (b) SNK-2. The age-depth model is developed by *RBACON v.2.2*. The red curve shows the 'best' estimated age by *RBACON*.

to appear abruptly in Zone-A (130–100 cm, 3200–1400 cal yr BP). Zone-B (100–65 cm, 1400–660 cal yr BP) is characterized by the dominance of *Quercus* (30–50 %) in the pollen assemblage and the first occurrence of *Avicennia germinans* pollen at 90 cm. Pollen grains of *Avicennia germinans* start to occur continuously upward from 75 cm (850 cal yr BP) (Fig. 6). In addition, charcoal fragments reach their highest concentration throughout the core in Zone-B. Zone-C (65–0 cm, 660 cal yr BP to present) is characterized by the dominance of Amaranthaceae in the pollen assemblage, while *Quercus* becomes less abundant (Fig. 6). Moreover, pollen grains of *Laguncularia racemosa* and *Rhizophora mangle* start to occur continuously at

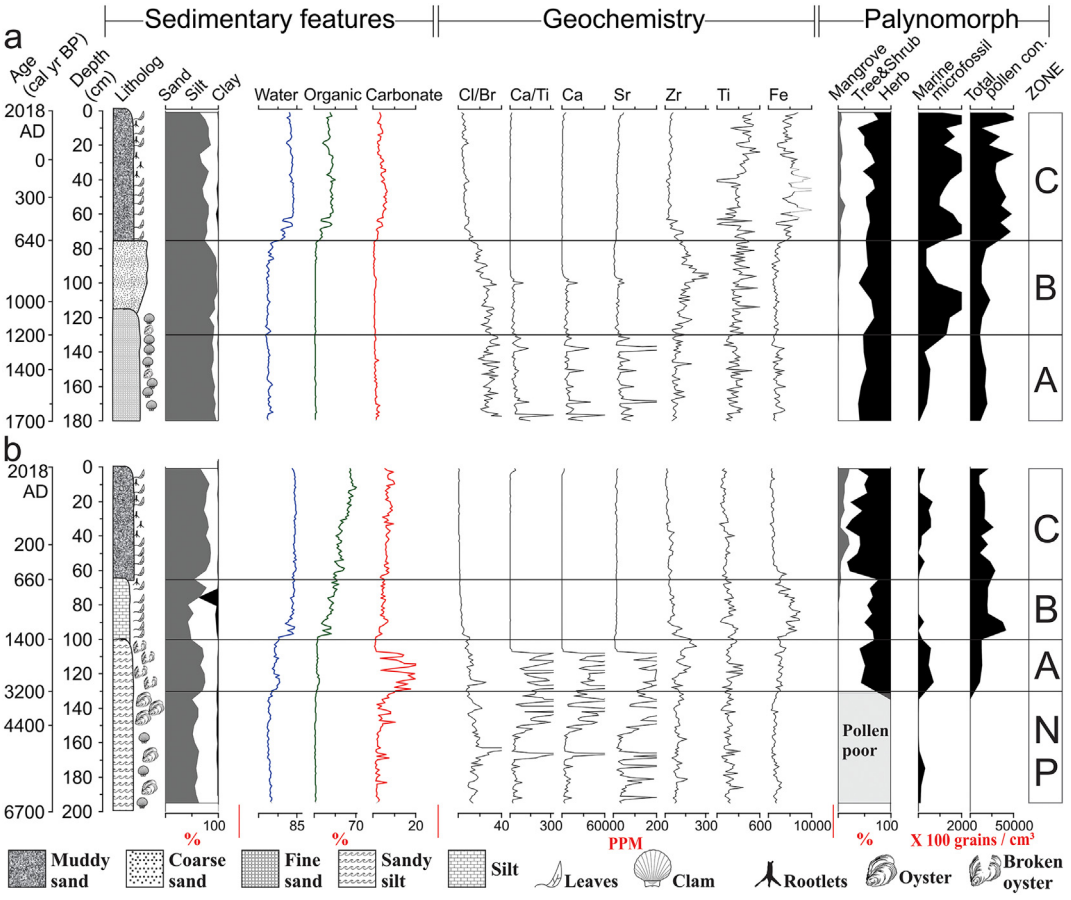

Fig. 4. Multi-proxy diagram summarizing (from left to right): the inferred chronology by the Bayesian model, sedimentary, geochemical, and palynological results of core (a) CK-2 and (b) SNK-2.

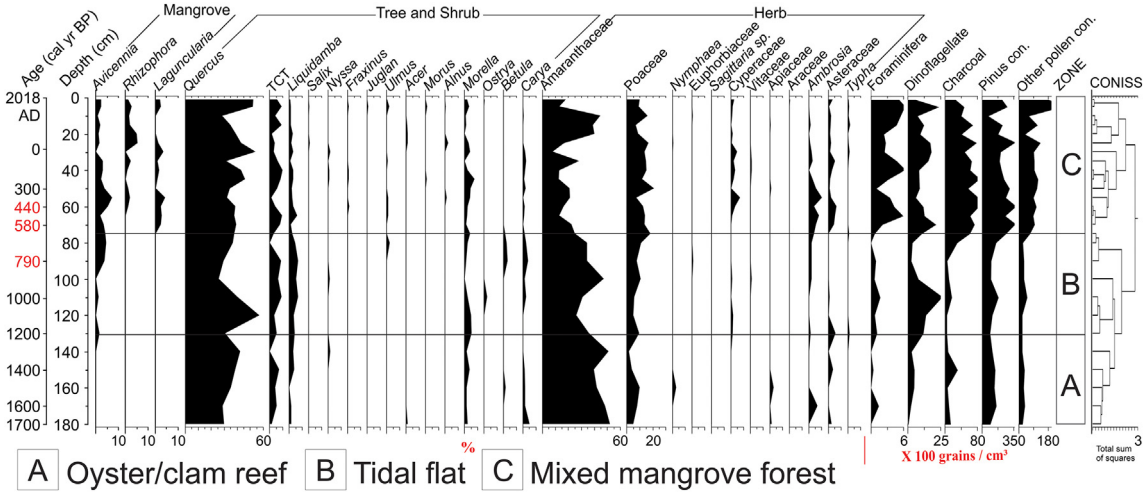

Fig. 5. Pollen diagram of core CK-2. The continuous appearance of *Avicennia germinans, Laguncularia racemosa,* and *Rhizophora mangle* pollen started at 790, 580, and 440 cal yr BP, respectively.

65 (660 cal yr BP) and 55 cm (460 cal yr BP), respectively (Fig. 5). In addition, foraminifera linings and dinoflagellate tests become more abundant throughout Zone-C.

4. Discussion

4.1. Geomorphological and ecological transformation at Atsena Otie key

The multi-proxy data indicate that our study area was undergoing shoreline progradation during the late Holocene (~1700 cal yr BP to present), marked by the stratigraphic changes from shell beds to organic-rich sediments in both cores (Fig. 4). In core CK-2, the bottom section (Zone-A) is characterized by abundant oyster and clam shells, as well as high values of marine indicators (e.g., Ca/Ti, Ca, and Sr) (Ramírez-Herrera et al., 2012; Yao and Liu, 2018; Williams et al., 2022). Very few charcoal fragments and high values of Cl/Br ratio also indicate a marine environment between ~1700 and 1200 cal yr BP (Liu et al., 2014; Yao et al., 2020b) (Fig. 4). Such settings highly resemble the oyster and clam reefs surrounding the Cedar Keys National Wildlife Refuge at the present day, suggesting the coring site on Atsena Otie Key was likely an oyster/clam reef prior to ~1200 cal yr BP. The pollen assemblage, characterized by abundant arboreal pollen taxa (e.g., *Quercus* and *Pinus*) (Fig. 5), also highly resembles the maritime forests (dominated by Slash Pine, Sand Pine, and shrubby oak) surrounding the refuge today (Field, 1991). The multi-proxy data show that the modern landscape near the Cedar Keys has been established since at least ~1200 cal yr BP.

Zone-B (~1200–640 cal yr BP) marks the establishment of mangroves on Atsena Otie Key (Fig. 4). The gradual decrease in the number of shells and salinity (indicated by Cl/Br ratio) points to a decrease in marine influence (Fig. 4). In addition, the grain size is increasing upward, suggesting an increase in energy flow (Fig. 4). Together, the above evidence indicates a transition from an oyster/shell reef to a sandy flat on Atsena Otie Key. More importantly, the pollen record shows that *Avicennia germinans* pollen (~4 %) started to consistently appear from 790 cal yr BP (Fig. 5). Studies from across the globe have shown that *Laguncularia* and *Avicennia* are insect-pollinated, and their pollen are typically under-represented in the pollen rain (Ellison, 2002; Yao et al., 2015; Yao and Liu, 2017). A low percentage (<5 %) of these taxa in the modern pollen rain has been reported from mangrove forests dominated by *Laguncularia* and *Avicennia* (Behling, 1993;

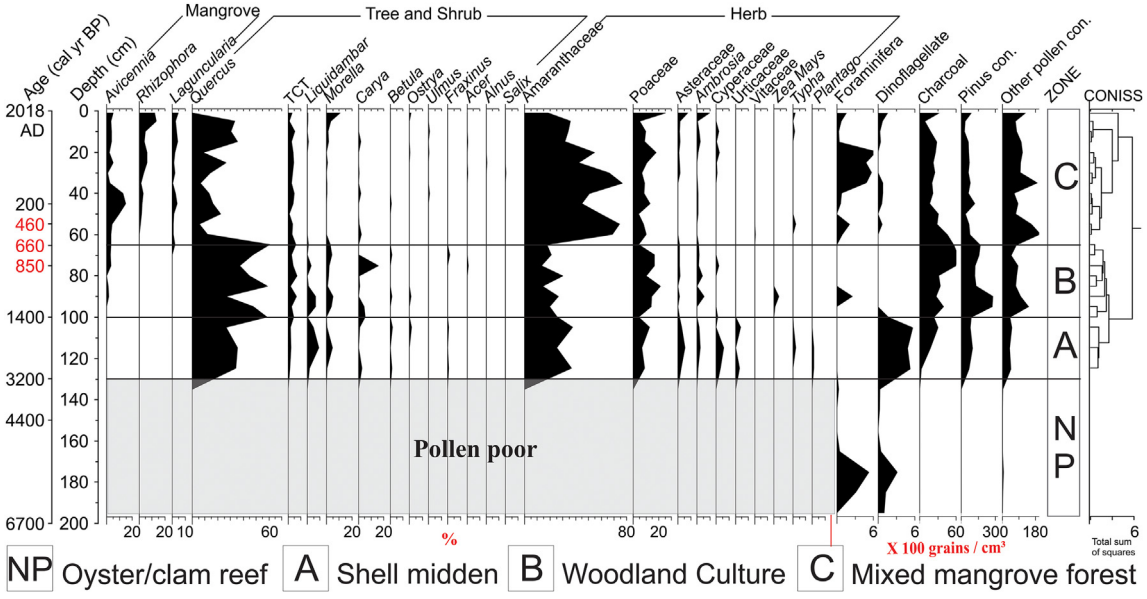

Fig. 6. Pollen diagram of core SNK-2. The continuous appearance of *Avicennia germinans, Laguncularia racemosa,* and *Rhizophora mangle* pollen started at 850, 660, and 460 cal yr BP, respectively.

Urrego et al., 2009, 2010). Hence, a mature mangrove forest dominated by *Avicennia germinans* has likely formed on Atsena Otie Key since ~790 cal yr BP. Collectively, considering mangrove trees usually grow in coastal or intertidal areas, our study area was transitioning from an oyster/clam reef to a tidal flat occupied by *Avicennia germinans* from ~1200 to 640 cal yr BP.

In Zone-C (~640 cal yr BP to present), pollen grains of *Laguncularia* and *Rhizophora* started to appear continuously from 70 cm and 60 cm (Fig. 5), marking their establishment on Atsena Otie Key since ~580 and 440 cal yr BP, respectively (Fig. 1c). In addition, the substrate of Zone-C is characterized by finer-grained sediments, while the overall pollen concentration, organic content, and Fe abundance increase substantially (Fig. 4). Such shifts in the sedimentary and geochemical features indicate a change from a high-energy (e.g., subtidal or intertidal flat exposed to the action of waves and currents) to a more stable terrestrial environment with lower energy flow (muddy intertidal flat) (Simard et al., 2006; You, 2008; Yao et al., 2021). The pollen assemblage highly resembles the mature mangrove swamp forests occupying the Florida Gulf coast today (Willard et al., 2004; van Soelen et al., 2012; Yao et al., 2015; Yao and Liu, 2017). Thus, Zone-C marks the seaward expansion of the mangrove forests as the shoreline prograded around Atsena Otie Key during the last ~600 years.

Moreover, charcoal fragments, Asteraceae (including *Ambrosia*), Cyperaceae, and Poaceae also become more abundant over the last ~600 years (Zone-C; Fig. 5). Charcoal fragments are usually associated with wood burning, while Asteraceae (especially *Ambrosia*) are early-successional plants associated with modification and destruction of natural vegetation for farmland, settlement, and other human activities (McAndrews, 1988; O'Neill Sanger et al., 2021). The above evidence indicates increasing human activity on the island during the past few centuries. Coincidentally, historical documents show that the Spanish have attempted to settle on vast lands along the Florida peninsula from the Keys to the Panhandle since the early 16th century (Lyon, 1981). Thus, it is reasonable to infer that Zone-C also marks the arrival of the Spanish colonial near Cedar Keys. It is also worth noting that among the Poaceae pollen grains present in Zone-C many are notably larger (>40 μm) than the pollen of typical wild or marsh grasses (Fig. 7c&d), which typically fall within the size

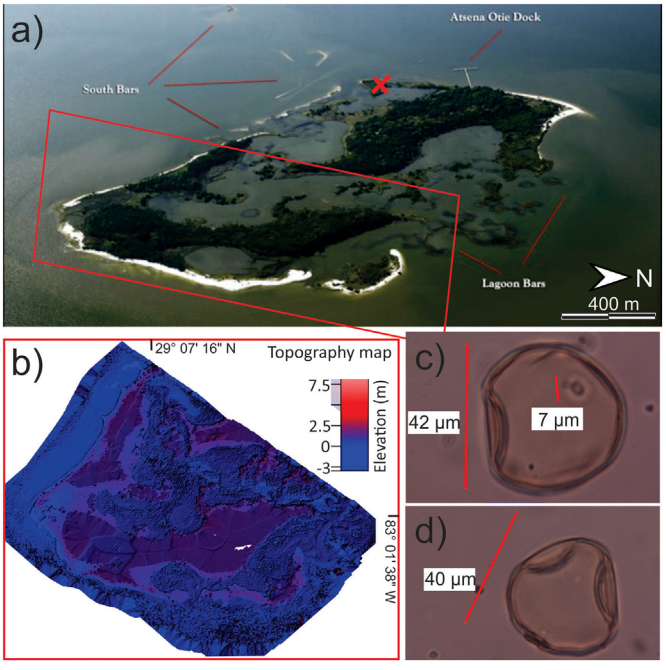

Fig. 7. (a) aerial photo (credited to Tommy Thompson) and (b) digital elevation model of Atsena Otie Key; (c) & (d) photos of *Zizania aquatica* pollen from Zone-C in core CK-2. The red cross in (a) marks the location of core CK-2, and the red rectangle shows the area presented in the digital terrain model in (b). Due to its proximity to a nearby airport, we were unable to produce digital elevation model using a UAV for the west side of the island where our coring site is located.

range of domesticated rice (*Oryza sativa*) pollen (Liu et al., 2018, 2021), though they are smaller than the pollen of maize (*Zea mays*) (Fearn and Liu, 1995). However, Cedar Keys lies outside of the distribution limits of wild rice species (*Oryza* spp.) (Ali et al., 2010; Stein et al., 2018) but is within the southern ranges of wild rice (*Zizania aquatica*) (Oelke, 1993; Porter, 2019). While it is possible that the Woodland native people in Cedar Keys may have harvested wild rice and used it in their diet in view of its importance as a staple food in the Great Lakes region (McAndrews, 1969; Lee et al., 2004), it is questionable whether the insular and coastal environment on Atsena Otie Key could provide sufficient freshwater or fluvial habitats to sustain the growth of *Zizania aquatica*. Given the dearth of information concerning the utilization of wild rice in areas outside of the Great Lakes region, including the Gulf Coast, more work needs to be done to verify the source of these relatively large Poaceae pollen grains.

In sum, the multi-proxy record of core CK-2 indicates a seaward expansion of Atsena Otie Key since ~1700 cal yr BP. Sediment accretion likely exceeded the rate of sea-level rise due to the deacceleration of the sea-level rise during the late Holocene (0.4 mm/yr) (Parkinson, 1989; Wanless et al., 1994), hence, transforming the oyster/clam reef at our coring site on Atsena Otie Key to a tidal flat occupied by *Avicennia germinans* at ~1200 cal yr BP (Figs. 4 and 5). The expansion of mangroves likely further facilitated the sediment accretion by trapping more fine grain sediments and in situ peat accumulation. Thus, more mangroves colonized the tidal flats and formed the mixed mangrove swamp at ~640 cal yr BP. Finally, the arrival of the Spanish Colonization marked the formation of the modern landscape on Atsena Otie Key.

4.2. The woodland native culture on seahorse key

Seahorse Key revealed a more intriguing and complex natural and anthropogenic history than Atsena Otie Key, especially the geomorphic histories of the two islands were very different. In core SNK-2, although the bottom section (Zone-NP, ~6700–3200 cal yr BP) exhibits similar sedimentary and geochemical characteristics as those in core CK-2 (Zone-A, ~1700–1200 cal yr BP), the former was deposited much earlier than the latter (Fig. 4). In particular, very few pollen grains (< 50 per sample) were recorded in each of the pollen samples from Zone-NP (Fig. 6). Previous studies have documented that the climate during the mid-Holocene was drier than today in Florida (Donders et al., 2005; Lodge, 2010; van Soelen et al., 2012). For example, the Gulf Coast of south Florida was occupied by marl prairies (short-hydroperiod marsh) at ~5000 cal yr BP (Parkinson, 1989; Yao et al., 2015; Yao and Liu, 2017). Thus, due to the drier climate, the dense maritime forests likely had not formed in the vicinity of the Cedar Keys; thus, few arboreal pollen grains were registered prior to ~3200 cal yr BP. Moreover, Zone-NP in SNK-2 contains an assortment of more intact oyster and clam shells (Fig. 3b), no charcoal, and very few grains of marsh pollen taxa (e.g., graminoids and sedges) (Fig. 6), suggesting that the study area was not vegetated prior to ~3200 cal yr BP. Thus, the multi-proxy record reveals a different landscape near the Cedar Keys during the middle to late Holocene than that of the present day, and the entire Seahorse Key (or the majority of the island) was an oyster/clam reef at that time.

Above this barren section, arboreal and marsh pollen taxa abruptly appear in Zone-A in SNK-2 (~3200–1400 cal yr BP) and the shell assemblage contains many broken shells (Fig. 3&6). The abrupt change in pollen and shell assemblages may suggest a hiatus between Zone-NP and Zone-A, and the shell harsh suggests human consumption (Saunders and Russo, 2011). It is remarkable that shell middens built by Native Americans have been discovered ~10 miles to the north of our study area (Saunders and Russo, 2011), we believe Zone-A represents a shell midden left by the Woodland people, a prehistoric native culture occurring in the eastern part of continental North America over 1000 years ago (Kelly et al., 1984; Wallis, 2008). According to archeological evidence from across the Atlantic and Gulf coasts of Florida, the Woodland people constructed shell middens as the base of their settlements (Wallis, 2008; Wallis and McFadden, 2019). Human activities might have removed some surficial sediments from the

site, thereby resulting in a hiatus between Zone-NP and Zone-A (Fig. 6). Moreover, the Woodland people also preferred to settle in backbay and more protected areas (Wallis and McFadden, 2019), which correspond to the environmental settings where core SNK-2 were taken (Fig. 8a-c). Thus, the chronology, shell assortment, and environmental settings of Zone-A are consistent with a shell midden left by the Woodland people.

More importantly, pollen grains of *Zea mays* (maize) were found exclusively in 90 and 95 cm (1260–1160 cal yr BP) in Zone-B (Fig. 8d&e), where the grain-size of the sediment becomes much finer (Fig. 4b). Aside from harvesting shell and fish, the Woodland culture was also characterized by raising corn among other crops such as quinoa (*Chenopodium quinoa*) (Region, 2000; Boyd and Surette, 2010), and the finer-grained soil is a typical feature associated with prehistoric human settlements around the globe (Liu et al., 2018, 2021; Zhao et al., 2022). Thus, the pollen and sedimentary features of Zone-B are also in line with a Woodland settlement built on Seahorse Key.

Zone-C (~660 cal yr BP to present) is characterized by distinct changes in the multi-proxy record, when mangrove pollen of all three species start to occur continuously (Fig. 6); herbaceous pollen become the dominant taxa (Fig. 4b); and the sediment changes to a muddy sand with high organic content (Fig. 3b). Such changes mark another distinct shift in the landscape – likely from Woodland settlement to mixed mangrove forest. Moreover, the timeline of this transition is in line with the arrival of the Spanish Colonization around the 1490s CE (~460 cal yr BP) (Fig. 5). Considering all the evidence, we believe the multi-proxy dataset of the two cores documents the demise of the Woodland Culture near Cedar Keys, where a once thriving Native community on Seahorse Key was replaced by a natural coastal ecosystem dominated by mangroves, marsh vegetation, and weeds starting about 500–600 years ago. Whether this cultural demise was caused by direct conflicts with the European colonizers, disease and mortality brought on by the European contact, or environmental changes driven by natural processes such as hurricanes remains to be investigated. However, it is clear that the prehistoric settlement was abandoned several centuries ago, and the site is overgrown with *Avicennia* trees in a mangrove forest today. In sum, the proxy record of core SNK-2 indicates that the coring site on Seahorse Key changed from an oyster/clam reef to a mixed mangrove forest (Fig. 6), while the organic content increases and the salinity decreases from the bottom to the top of the core (Fig. 4b). Such sedimentary and geochemical transformation marks a shoreline progradation on Seahorse Key, highly resembling that of Atsena Otie Key. More importantly, *Avicennia germinans*, *Laguncularia racemosa*, and *Rhizophora mangle* started to continuously occur around 850, 660, and 460 cal yr BP, respectively (Fig. 6). Thus, the successional order and the establishment timeline of all three mangrove species are also similar on the two islands (Figs. 5 and 6).

4.3. Poleward mangrove migration and climate anomalies

During the Holocene, mangroves were first established in the continental United States in south Florida (~25°N) ~4000 cal yr BP (Yao and Liu, 2017; Jones et al., 2019). However, it took them over 3000 years to reach Cedar

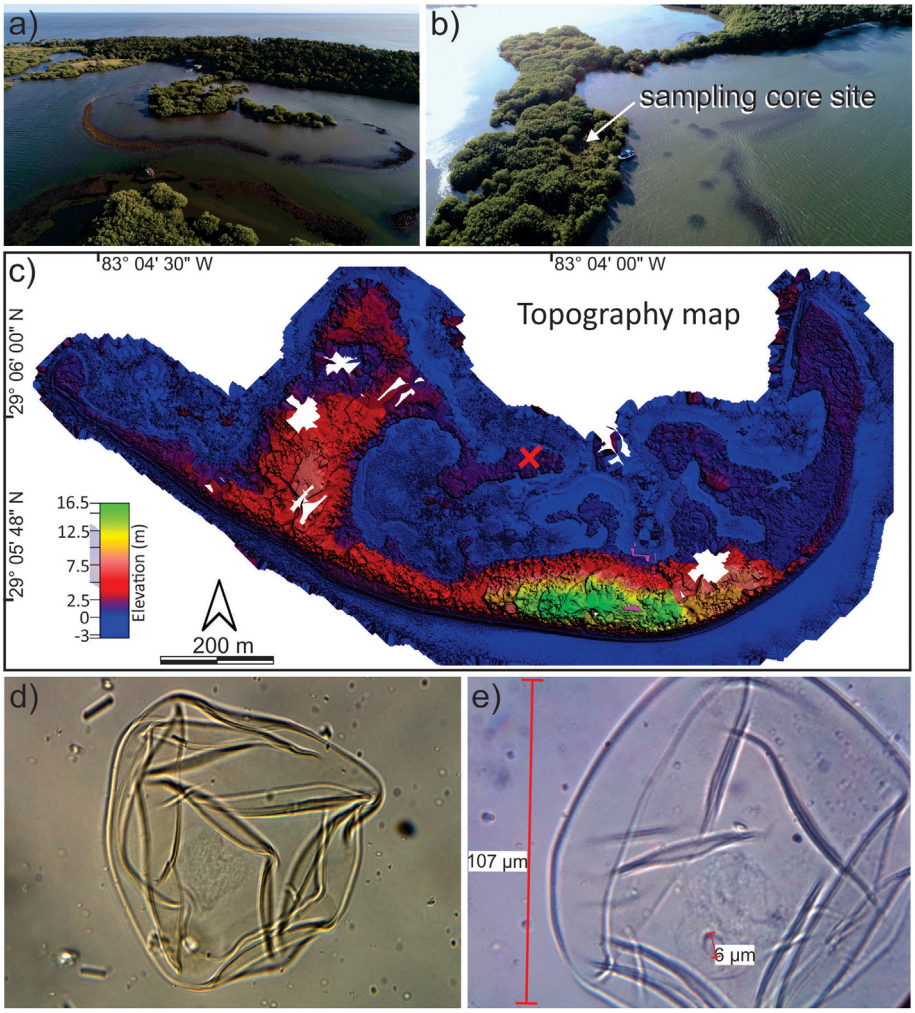

Fig. 8. (a) & (b) aerial photos of the coring site on Seahorse Key, (c) digital elevation model of Seahorse Key, and (d) & (e) photos of *Zea mays* (corn) pollen from Zone-b in core SNK-2. The red cross in (c) marks the location of core SNK-2.

Keys (~29°N; Fig. 9). Moreover, the current disjunct distribution of mangroves, particularly *Avicennia germinans*, along the GOM coast (Fig. 1a; Yao et al., 2022b) could be the result of either an expansion or a contraction of the species range over time. On a regional scale, the processes that can produce disjunct distributions include climate anomalies, environmental changes (e.g., RSL and salinity), and anthropogenic activities, among others (Tallis, 1991). On a global scale, the latitudinal range of mangroves is regulated by macro-climatic and physical factors such as winter freezes (threshold = − 4 °C), sea-level rise (threshold = 6.1 mm/yr), and low precipitation (threshold = 780 mm/yr) (Blasco et al., 1996; Osland et al., 2017; Ward et al., 2016; Saintilan et al., 2020). Thus, analyzing the forces operating on a macro and regional scale is vital to understanding the distribution of mangroves in the continental Americas.

Across the northeastern GOM, the slow RSL rise (0.4 mm/yr) (Parkinson, 1989; Wanless et al., 1994) and abundant rainfall (Donders et al., 2005) during the late Holocene were well below the thresholds that affect the survival of mangrove populations, thereby ruling out RSL variations and precipitation as factors limiting mangroves migration toward higher latitudes. On a local scale, mangroves usually proliferate on a muddy and silty substrate, where mangrove propagules can anchor their roots (Cohen et al., 2020a; Rodrigues et al., 2022; Yao et al., 2022b). At Cedar Keys, the grain-size analyses show that the sediment profiles consisted of silt, an ideal substrate for mangroves (Yao et al., 2015; Yao and Liu, 2018), since the mid-Holocene (Figs. 3b and 4b). Therefore, the substrate was likely not a limiting factor either. In addition, studies from south Brazil have shown that low-salinity environment (< 6 ‰) could sometimes eliminate the competitive advantage (i.e., tolerance to high salinity) of mangroves over marsh species (Cohen et al., 2020a). However, this possibility is rejected as well because our study area was occupied by oyster/clam reef (thrive in salinity ~14–28 ‰) during the mid-Holocene (Figs. 3 and 4). Moreover, the global mangrove biogeography shows a latitudinal limitation, regulated by a temperature threshold (Alongi, 2015; Osland et al., 2017; Cavanaugh et al., 2018). Therefore, it is reasonable to propose that temperature is likely the key factor regulating the migration of mangroves beyond their current sub-range limit in North America.

Furthermore, the establishment of black mangrove (*Avicennia germinans*) near Cedar Keys occurred during the MCA (~1050 to 750 cal yr BP) (Fig. 9b), a warm climate anomaly across the North Atlantic Basin (Fig. 9d; Kerr, 2000; Mann et al., 2009), especially from the northern GOM region (Fig. 9c; Esper et al., 2002; Richey et al., 2007). More importantly, the timeline of this mangrove expansion also coincides with that in South America, where mangroves established at their sub-range limit (26°S) in south Brazil ~870 cal yr BP (Fig. 9a; Rodrigues et al., 2022). Thus, it is reasonable to believe that during the MCA, when the winter temperature was relatively mild, mangroves migrated to their sub-range limits in North (~29°N) and South America (~26°N) from the lower latitudes as the RSL was near the modern level and the sea-level rise rates were stabilized in the last millennium (Cohen et al., 2014, 2020a; Rodrigues et al., 2021; Toscano and Macintyre, 2003a, 2003b). Overall, the patterns of poleward mangrove migration in North and South America were synchronized during the last millennium, and both were likely triggered by the MCA (Fig. 9).

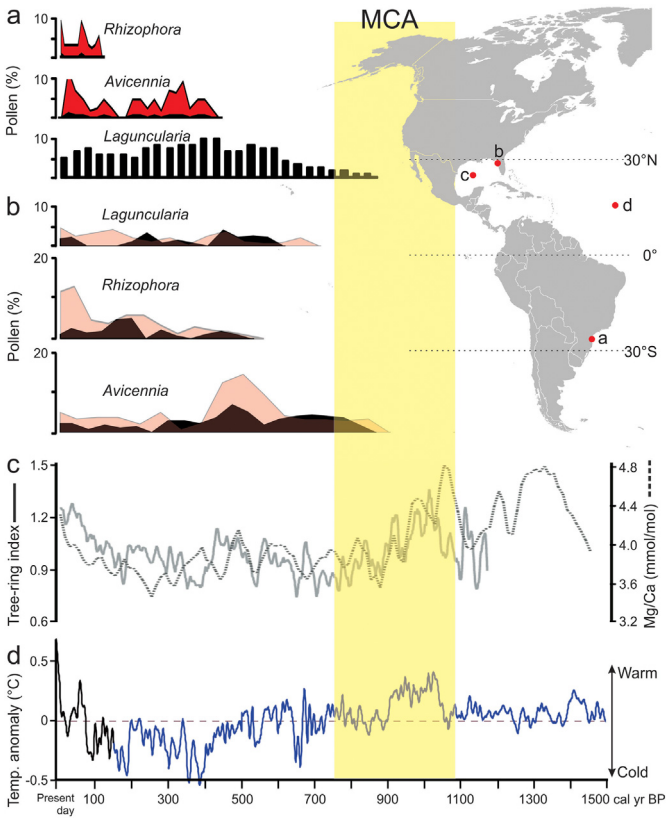

Fig. 9. Mangrove pollen record from (a) São Francisco do Sul Bay in south Brazil (26°S) compared with (b) core CK-2 (black silhouette) and SNK-2 (red shade), (c) SST record of northern GOM based on Mg/Ca analysis of foraminifera (dash line; Richey et al., 2007) and tree-ring record of the Northern Hemisphere temperature (solid line; Esper et al., 2002), and (d) SST record over the North Atlantic Ocean (Kerr, 2000). The yellow shade marks the MCA (~1050–750 cal yr BP).

4.4. Adaptation of different mangrove species at different latitudes

Although winter temperature is the main factor that regulates the mangrove distribution on a continental scale, on a regional scale, it is necessary to consider the peculiarities of potential mangrove habitats at different latitudes. As long as the winter climate is mild enough for mangrove establishment, their presence or absence will depend on an equilibrium involving the interplay among local factors such as river discharge, salinity, sea level, and local hydrodynamic conditions related to tides, waves, and littoral currents, as well as sediment type and the rate of sediment supply (Cohen et al., 2020b; Saintilan et al., 2020; Woodroffe and Grindrod, 1991).

Generally speaking, *Avicennia germinans* and *Laguncularia racemosa* are more tolerant of low temperatures than *Rhizophora mangle* (Stuart et al., 2007; Tomlinson, 2016; Osland et al., 2020). Consequently, near the mangrove latitudinal range limits in North and South America, where winter freezes are possible but rare, *Avicennia* and *Laguncularia* established earlier than *Rhizophora* (Fig. 9). However, their individual biogeography differed in the two continents. For example, along the Gulf of Mexico coast in North America, *Avicennia* dominates the mangrove colonies (Osland et al., 2017; Yao et al., 2022b). In South America, *Laguncularia* was usually established before *Avicennia* near the austral mangrove range limit during the middle to late Holocene (Cohen et al., 2020a; França et al., 2019; Rodrigues et al., 2022). Thus, it is likely that the two mangrove species in the two continents evolved different physiological adaptations to frequent winter freezes while they were migrating toward the higher latitudes (Oliveira, 2005; Stuart et al., 2007; Quisthoudt et al., 2012; Osland et al., 2017). As a result of these ecophysiological differences, the North American *Avicennia germinans* populations are more tolerant to winter freezes than their South American counterparts; and vice versa for *Laguncularia*.

Furthermore, the mangrove biogeography also differs in the lower latitudes. Using south Florida as an example, where the minimum winter temperature (>0 °C) is well above the physiological thresholds for mangroves (− 4 °C), *Rhizophora* was usually established first along the coast, while *Avicennia* arrived the latest among the three (Yao and Liu, 2017; Jones et al., 2019). Since *Rhizophora* has prop roots and hardy propagules, they are more adapted to high-energy environments (Ellison, 2002; Alongi, 2015). It is reasonable to infer that these physiological advantages facilitated the colonization of *Rhizophora* along the dynamic coasts of south Florida. However, in the same region, studies also found that *Laguncularia* was typically the pioneer colonizer in low-salinity environments during the Holocene (Yao and Liu, 2017, 2018), likely due to their

physiological adaptation to the upper intertidal and low-salinity habitats (Koundouri et al., 2017; Vogt et al., 2012; Zimmer, 2022). Thus, the adaptation of different mangrove species at different latitudes is likely more complicated than a singular threshold. More specifically, at the higher latitudes, wherever the substrate and salinity conditions are suitable for mangrove establishment, winter freezes would play a more predominant role in limiting the poleward mangrove expansion. By contrast, at lower latitudes, where the winter is mild and freezes are absent or rare, the local hydrodynamic condition, coastal morphology, and salinity would become the primary control of the establishment of mangroves.

5. Conclusion

This study documents the geomorphological and ecological transformation of Cedar Keys, FL, the mangrove sub-range limit in North America (Fig. 1) during the middle to late Holocene. The multi-proxy records from two islands show that the Medieval Climate Anomaly favored the mangrove establishment in the study region, with *Avicennia, Laguncularia*, and *Rhizophora* arriving in the ~12th (790–850 cal yr BP), ~14th (580–660 cal yr BP), and ~ 16th century (440–460 cal yr BP), respectively. The sequence of arrival and establishment of the three mangrove species are consistent with their different degrees of tolerance to low temperatures, thereby suggesting a delayed response to the warmer climate during the MCA in the early part of the last millennium (Fig. 9). Following this trend, mangroves and marsh vegetation have covered the abandoned site of the Woodland people on Seahorse Key since the 15th century. Under the projected Anthropocene warming trend in the 21st century, it is reasonable to conclude that mangroves, especially *Avicennia germinans*, will continue to migrate into more temperate coastal zones in North America. The Holocene history of mangrove colonization at Cedar Keys suggests that the colonization of *Rhizophora* and *Laguncularia* along the northern GOM coast will be an inevitable process in the future. In particular, a rapidly rising sea level trend is likely to facilitate marine incursion into coastal marshes, creating the physio-chemical condition favorable for mangrove establishment, further accelerating the mangrove expansion along the northern GOM coast. This study reveals the Holocene history of mangroves at a critical location along their migratory route from south to north Florida. The parallelism between the vegetation histories at Cedar Keys and other mangrove study sites in North and South America can provide insight into the climatic and environmental thresholds controlling the distribution and abundance of mangroves in the Americas.

Author contributions

Q.Y conceived the hypothesis, led the fieldwork, and wrote the manuscript.

K.B.L conceived the hypothesis, assisted in writing and editing, and led the project.

E.R led the multi-proxy analyses.

D.D·F led the short-lived isotopic dating.

M.C. led the spatial-temporal analysis and assisted in writing and editing.

Correspondence and requests for materials should be addressed to Qiang Yao at qyao4@lsu.edu

Data availability

All datasets produced in this article will be stored at the Neotoma Paleoecology Database (https://www.neotomadb.org) upon publication and accessible to the public for free.

Declaration of competing interest

The authors declare that they have no known competing financial interests or personal relationships that could have appeared to influence the work reported in this paper.

Acknowledgments

We thank Florida Department of Wildlife and Fisheries for their assistance in securing the research permit. We also thank all the current and past members of the LSU Global Change and Coastal Paleoecology Laboratory for their assistance. This study was funded by the U.S. National Science Foundation (NSF #1759715), State Key Laboratory of Marine Geology (MGK-1911), Brazilian National Council for Technology and Science (CNPq 07497/2018-6, 403239/2021-4), Research Funding Agency of the State of São Paulo (FAPESP 2020/13715-1).

Appendix A. Supplementary data

Supplementary data to this article can be found online at https://doi.org/10.1016/j.scitotenv.2022.160189.

References

Ali, M.L., Sanchez, P.L., Yu, S.B., Lorieux, M., Eizenga, G.C., 2010. Chromosome segment substitution lines: a powerful tool for the introgression of valuable genes from Oryza wild species into cultivated rice (O. sativa). Rice 3 (4), 218–234.

Alongi, D.M., 2015. The impact of climate change on mangrove forests. Curr.Clim.Chang.Rep. 1 (1), 30–39. https://doi.org/10.1007/s40641-015-0002-x.

Armitage, A.R., Highfield, W.E., Brody, S.D., Louchouarn, P., 2015. The contribution of mangrove expansion to salt marsh loss on the Texas Gulf Coast. PLoS One 10, e0125404.

Barbier, E.B., Hacker, S.D., Kennedy, C., Koch, E.W., Stier, A.C., Silliman, B.R., 2011. The value of estuarine and coastal ecosystem services. Ecol. Monogr. 81, 169–193.

Behling, H., 1993. Untersuchungen zur spätpleistozänen und holozänen Vegetations- und Klimageschichte der tropischen Küstenwälder und der Araukarienwälder in Santa Catarina (Südbrasilien). Dissertationes Botanicae 206. J. Cramer, Cramer, Berlin, Stuttgart. https://doi.org/10.1016/S0034-6667(97)00044-4.

Biasutti, M., Sobel, A.H., Camargo, S.J., Creyts, T.T., 2012. Projected changes in the physical climate of the Gulf Coast and Caribbean. Clim. Chang. 112 (3–4), 819–845.

Blaauw, M., Christen, J.A., 2011. Flexible paleoclimate age-depth models using an autoregressive gamma process. Bayesian Anal. 6 (3), 457–474.

Blasco, F., Saenger, P., Janodet, E., 1996. Mangroves as indicators of coastal change. Catena 27 (3–4), 167–178. https://doi.org/10.1016/0341-8162(96)00013-6.

Box, E.O., Crumpacker, D.W., Hardin, E.D., 1993. A climatic model for location of plant species in Florida, U.S.A. J. Biogeogr. 20, 629. https://doi.org/10.2307/2845519.

Boyd, M., Surette, C., 2010. Northernmost precontact maize in North America. Am. Antiq. 75 (1), 117–133.

Bozi, B.S., Figueiredo, B.L., Rodrigues, E., Cohen, M.C., Pessenda, L.C., Alves, E.E., de Souza, A.V., Bendassolli, J.A., Macario, K., Azevedo, P., Culligan, N., 2021. Impacts of sea-level changes on mangroves from southeastern Brazil during the Holocene and Anthropocene using a multi-proxy approach. Geomorphology 390, 107860.

Cavanaugh, K.C., Kellner, J.R., Forde, A.J., Gruner, D.S., Parker, J.D., Rodriguez, W., Feller, I.C., 2014. Poleward expansion of mangroves is a threshold response to decreased frequency of extreme cold events. Proc. Natl. Acad. Sci. 111 (2), 723–727.

Cavanaugh, K.C., Osland, M.J., Bardou, R., Hinojosa-Arango, G., López-Vivas, J.M., Parker, J.D., Rovai, A.S., 2018. Sensitivity of mangrove range limits to climate variability. Glob. Ecol. Biogeogr. 27 (8), 925–935. https://doi.org/10.1111/geb.12751.

Cavanaugh, K.C., Dangremond, E.M., Doughty, C.L., Williams, A.P., Parker, J.D., Hayes, M.A., Rodriguez, W., Feller, I.C., 2019. Climate-driven regime shifts in a mangrove–salt marsh ecotone over the past 250 years. Proc. Natl. Acad. Sci. 116 (43), 21602–21608.

Clark, P.U., Dyke, A.S., Shakun, J.D., Carlson, A.E., Clark, J., Wohlfarth, B., McCabe, A.M., 2009. The last glacial Maximum. Science 325 (5941), 710–714. https://doi.org/10.1126/science.1172873.

Cohen, M.C.L., França, M.C., de Fátima, Rossetti D., Pessenda, L.C.R., Giannini, P.C.F., Lorente, F.L., Macario, K., 2014. Landscape evolution during the late Quaternary at the Doce River mouth, Espírito Santo State, southeastern Brazil. Palaeogeogr. Palaeoclimatol. Palaeoecol. 415, 48–58. https://doi.org/10.1016/j.palaeo.2013.12.001.

Cohen, M.C.L., Rodrigues, E., Rocha, D.O.S., Freitas, J., Fontes, N.A., Pessenda, L.C.R., de Souza, A.V., Gomes, V.L.P., França, M.C., Bonotto, D.M., Bendassolli, J.A., 2020a. Southward migration of the austral limit of mangroves in South America. Catena 195, 104775. https://doi.org/10.1016/j.catena.2020.104775.

Cohen, M.C.L., Figueiredo, B.L., Oliveira, N.N., Fontes, N.A., França, M.C., Pessenda, L.C.R., de Souza, A.V., Macario, K., Giannini, P.C.F., Bendassolli, J.A., Lima, P., 2020b. Impacts of Holocene and modern sea-level changes on estuarine mangroves from northeastern Brazil. Earth Surf. Process. Landf. 45, 375–392. https://doi.org/10.1002/esp.4737.

Cohen, M.C.L., de Souza, A.V., Liu, K.-B., Rodrigues, E., Yao, Q., Pessenda, L.C.R., Rossetti, D., Ryu, J., Dietz, M., 2021. Effects of beach nourishment project on coastal geomorphology and mangrove dynamics in Southern Louisiana, USA. Remote Sens. 13, 2688. https://doi.org/10.3390/RS13142688.

Cook-Patton, S.C., Lehmann, M., Parker, J.D., 2015. Convergence of three mangrove species towards freeze-tolerant phenotypes at an expanding range edge. Funct. Ecol. 29, 1332–1340.

Corbett, D.R., Walsh, J.P., 2015. 210 lead and 137 cesium. Handbook of Sea-level Research. John Wiley & Sons, Ltd. https://doi.org/10.1002/9781118452547.ch24.

Dittmar, T., Hertkorn, N., Kattner, G., Lara, R.J., 2006. Mangroves, a major source of dissolved organic carbon to the oceans. Glob. Biogeochem. Cycles 20. https://doi.org/10.1029/2005GB002570.

Donders, T.H., Wagner, F., Dilcher, D.L., Visscher, H., 2005. Mid- to late-Holocene El Niño-Southern Oscillation dynamics reflected in the subtropical terrestrial realm. Proc. Natl. Acad. Sci. U. S. A. 102 (10) 904 ± 10,908.

Ellison, A.M., 2002. Macroecology of mangroves: large-scale patterns and processes in tropical coastal forests. Trees 16 (2–3), 181–194. https://doi.org/10.1007/s00468-001-0133-7.

Esper, J., Cook, E.R., Schweingruber, F.H., 2002. Low-frequency signals in long tree-ring chronologies for reconstructing past temperature variability. Science 295, 2250–2254. https://doi.org/10.1126/science.1066208.

Fearn, M.L., Liu, K.B., 1995. Maize pollen of 3500 BP from southern Alabama. Am. Antiq. 60 (1), 109–117.

Field, D.W., 1991. Coastal Wetlands of the United States: An Accounting of a Valuable National Resource. Vol. 55. National Oceanic and Atmospheric Administration.

Figueiredo, B.L., Alves, I.C.C., Cohen, M.C., Pessenda, L.C., França, M.C., Francisquini, M.I., de Souza, A.V., Culligan, N., 2021. Climate, sea-level, and anthropogenic influences on coastal vegetation of the southern Bahia, northeastern Brazil, during the mid-late Holocene. Geomorphology 394, 107967.

França, M.C., Pessenda, L.C., Cohen, M.C., de Azevedo, A.Q., Fontes, N.A., Silva, F.B., de Melo Jr, J.C., Piccolo, M.D.C., Bendassolli, J.A., Macario, K., 2019. Late-Holocene subtropical mangrove dynamics in response to climate change during the last millennium. The Holocene 29 (3), 445–456.

Gilman, E.L., Ellison, J., Duke, N.C., Field, C., 2008. Threats to mangroves from climate change and adaptation options: a review. Aquat. Bot. 89, 237–250. https://doi.org/10.1016/j.aquabot.2007.12.009.

Goldberg, E.D., 1963. Geochronology with 210Pb. Radioactive Dating, pp. 121–131.

Grimm, E.C., 1987. CONISS: a FORTRAN 77 program for stratigraphically constrained cluster analysis by the method of incremental sum of squares. Comput. Geosci. 13 (1), 13–35. https://doi.org/10.1016/0098-3004(87)90022-7.

Grimm, E.C., Troostheide, C.D., 1994. Tilia 2.00, Program for Plotting Palynological Diagrams. Springfield, Illinois State Museum.

Haug, G.H., Hughen, K.A., Sigman, D.M., Peterson, L.C., Röhl, U., 2001. Southward migration of the intertropical convergence zone through the Holocene. Science 293 (5533), 1304–1308.

Hutchison, J., Manica, A., Swetnam, R., et al., 2014. Predicting global patterns in mangrove forest biomass. Conserv. Lett. 7, 233–240. https://doi.org/10.1111/conl.12060.

Jones, M.C., Wingard, G.L., Stackhouse, B., Keller, K., Willard, D., Marot, M., Landacre, B., E Bernhardt, C., 2019. Rapid inundation of southern Florida coastline despite low relative sea-level rise rates during the late-Holocene. Nat. Commun. 10 (1), 1–13.

Kauffman, J.B., Heider, C., Cole, T.G., et al., 2011. Ecosystem carbon stocks of micronesian mangrove forests. Wetlands 31, 343–352. https://doi.org/10.1007/s13157-011-0148-9.

Kelly, J.E., Finney, F.A., McElrath, D.L., Ozuk, S.J., 1984. Late woodland period. American Bottom Archaeology, pp. 104–127.

Kennedy, J.P., Pil, M.W., Proffitt, C.E., Boeger, W.A., Stanford, A.M., Devlin, D.J., 2016. Post-glacial expansion pathways of red mangrove, Rhizophora mangle, in the Caribbean Basin and Florida. Am. J. Bot. 103, 260–276.

Kerr, R.A., 2000. A North Atlantic climate pacemaker for the centuries. Science 288 (5473), 1984–1985.

Koundouri, P., Boulton, A.J., Datry, T., Souliotis, I., 2017. Ecosystem services, values, and societal perceptions of intermittent rivers and ephemeral streams. Intermittent Rivers Ephemer. Streams. Ecol. Manag., 455–476. https://doi.org/10.1016/B978-0-12-803835-2.00018-8.

Lee, G.A., Davis, A.M., Smith, D.G., McAndrews, J.H., 2004. Identifying fossil wild rice (Zizania) pollen from Cootes Paradise, Ontario: a new approach using scanning electron microscopy. J. Archaeol. Sci. 31 (4), 411–421.

Lisiecki, L.E., Jones, A.M., Rand, D., Lee, T., Lawrence, C.E., 2022. Comparing age model techniques for the last glacial cycle: a case study of ten Iberian Margin sediment cores. Quat. Sci. Rev. 287, 107559. https://doi.org/10.1016/J.QUASCIREV.2022.107559.

Little, E.L., 1978. Atlas of United States Trees: Florida (No. 1361). US Department of Agriculture, Forest Service.

Liu, K.B., McCloskey, T.A., Ortego, S., Maiti, K., 2014. Sedimentary signature of Hurricane Isaac in a Taxodium swamp on the western margin of Lake Pontchartrain, Louisiana, USA. Proceedings of the International Association of Hydrological Sciences. 367, pp. 421–428.

Liu, Y., Sun, Q., Fan, D., Dai, B., Ma, F., Xu, L., Chen, J., Chen, Z., 2018. Early to Middle Holocene Sea level fluctuation, coastal progradation and the Neolithic occupation in the Yaojiang Valley of southern Hangzhou Bay, eastern China. Quat. Sci. Rev. 189, 91–104.

Liu, Y., Deng, L., He, J., Zhao, X., Wang, H., Feng, D., Chen, J., Li, M., Sun, Q., 2021. Holocene geomorphological evolution and the Neolithic occupation in South Hangzhou Bay, China. Geomorphology 389, 107827.

Lodge, T.E., 2010. The Everglades Handbook: Understanding the Ecosystem. Second edition. CRC Press, Boca Raton, Florida.

Lyon, E., 1981. Spain's sixteenth-century North American settlement attempts: a neglected aspect. Fla.Hist.Q. 59 (3), 275–291.

Mann, M.E., Zhang, Z., Rutherford, S., Bradley, R.S., Hughes, M.K., Shindell, D., Ammann, C., Faluvegi, G., Ni, F., 2009. Global signatures and dynamical origins of the Little Ice Age and Medieval Climate Anomaly. Science 326 (5957), 1256–1260.

McAndrews, J.H., 1969. Paleobotany of a wild rice lake in Minnesota. Can. J. Bot. 47 (11), 1671–1679.

McAndrews, J.H., 1988. Human disturbance of North American forests and grasslands: the fossil pollen record. Veg.Hist. 673–697.

Miall, A.D., 1978. Facies types and vertical profile models in braided river deposits: a summary. In: Miall, A.D. (Ed.), Fluvial Sedimentology. Canadian Society of Petroleum Geologists, Calgary, pp. 597–604.

Miller, R., 1945. The heavy minerals of Florida beach and dune sands. Am. Mineral. 30, 65–75.

Montagna, P.A., Brenner, J., Gibeaut, J., Morehead, S., 2011. Coastal impacts. In: Schmandt, J., North, G.R., Clarkson, J. (Eds.), The Impact of Global Warming on Texas, Second edition University of Texas Press, Austin, Texas, USA, pp. 96–123.

NOAA CO-OPS, .. https://tidesandcurrents.noaa.gov/sltrends/sltrends_station.shtml?id = 8727520 Accessed May, 2022.

O'Neill Sanger, C.E., St-Jacques, J.M., Peros, M.C., Schwartz, K.A., 2021. Reconstructed high-resolution forest dynamics and human impacts of the past 2300 years of the Parc national de Mont-Orford, southeastern Québec,Canada. Holocene 31 (6), 1019–1032.

Oelke, E.A., 1993. Wild Rice: Domestication of a Native North American Genus. New crops. Wiley, New York, pp. 235–243.

Oliveira, V.F., 2005. Influência do estresse hídrico e salino na germinação de propágulos de Avicennia schaueriana Stapf e Leechman ex Moldenke e Laguncularia racemosa (L.) Gaertn. f. MS DissertationPrograma de Pós-Graduação em Botânica, Instituto de Pesquisas Jardim Botânico do Rio de Janeiro (JBRJ), Rio de Janeiro 92 pp.

Osland, M.J., Enwright, N., Day, R.H., Doyle, T.W., 2013. Winter climate change and coastal wetland foundation species: salt marshes vs. mangrove forests in the southeastern United States. Glob. Chang. Biol. 19 (5), 1482–1494.

Osland, M.J., Day, R.H., Hall, C.T., Brumfield, M.D., Dugas, J.L., Jones, W.R., 2017. Mangrove expansion and contraction at a poleward range limit: climate extremes and land-ocean temperature gradients. Ecology 98 (1), 125–137.

Osland, M.J., Grace, J.B., Guntenspergen, G.R., Thorne, K.M., Carr, J.A., Feher, L.C., 2019. Climatic controls on the distribution of foundation plant species in coastal wetlands of the conterminous United States: knowledge gaps and emerging research needs. Estuar. Coasts 42, 1991–2003.

Osland, M.J., Day, R.H., Hall, C.T., Feher, L.C., Armitage, A.R., Cebrian, J., Dunton, K.H., Randall Hughes, A., Kaplan, D.A., Langston, A.K., Macy, A., Weaver, C.A., Anderson, G.H., Cummins, K., Feller, I.C., Snyder, C.M., 2020. Temperature thresholds for black mangrove (Avicennia germinans) freeze damage, mortality, and recovery in North America: refining tipping points for range expansion in a warming climate. J. Ecol. 108, 654–665.

Osland, M.J., Stevens, P.W., Lamont, M.M., Brusca, R.C., Hart, K.M., Waddle, J.H., Langtimm, C.A., Williams, C.M., Keim, B.D., Terando, A.J., Reyier, E.A., 2021. Tropicalization of temperate ecosystems in North America: the northward range expansion of tropical organisms in response to warming winter temperatures. Glob. Chang. Biol. 27 (13), 3009–3034.

Osland, M.J., Hughes, A.R., Armitage, A.R., Scyphers, S.B., Cebrian, J., Swinea, S.H., Shepard, C.C., Allen, M.S., Feher, L.C., Nelson, J.A., O'Brien, C.L., 2022. The impacts of mangrove range expansion on wetland ecosystem services in the southeastern United States: current understanding, knowledge gaps, and emerging research needs. Glob. Chang. Biol. 28 (10), 3163–3187.

Parkinson, R.W., 1989. Decelerating Holocene sea-level rise and its influence on Southwest Florida coastal evolution: a transgressive/regressive stratigraphy. J. Sediment. Petrol. 59 (6), 960 ± 972.

Porter, R., 2019. Wildrice (Zizania L.) in North America: genetic resources, conservation, and use. North American Crop Wild Relatives. Volume 2. Springer, Cham, pp. 83–97.

Quisthoudt, K., Schmitz, N., Randin, C.F., Dahdouh-Guebas, F., Robert, E.M., Koedam, N., 2012. Temperature variation among mangrove latitudinal range limits worldwide. Trees 26 (6), 1919–1931. https://doi.org/10.1007/s00468-012-0760-1.

Ramírez-Herrera, M.T., Lagos, M., Hutchinson, I., Kostoglodov, V., Machain, M.L., Caballero, M., Goguitchaichvili, A., Aguilar, B., Chagué Goff, C., Goff, J., Ruiz-Fernández, A.C., 2012. Extreme wave deposits on the Pacific coast of Mexico: tsunamis or storms? A multi-proxy approach. Geomorphology 139, 360–371.

Region, M.R., 2000. Regional variations in plant use strategies in the Midwest during the Late Woodland. Late Woodland Societies: Tradition And Transformation Across the Midcontinent, p. 37.

Richey, J.N., Poore, R.Z., Flower, B.P., Quinn, T.M., 2007. 1400 yr multiproxy record of climate variability from the northern Gulf of Mexico. Geology 35 (5). https://doi.org/10.1130/G23507A.1.

Robbins, J.A., Edgington, D.N., 1975. Determination of recent sedimentation rates in Lake Michigan using Pb-210 and Cs-137. Geochim. Cosmochim. Acta 39 (3), 285–304.

Rodrigues, E., Cohen, M.C., Liu, K.B., Pessenda, L.C., Yao, Q., Ryu, J., Rossetti, D., de Souza, A., Dietz, M., 2021. The effect of global warming on the establishment of mangroves in coastal Louisiana during the Holocene. Geomorphology 381, 107648.

Rodrigues, E., Cohen, M.C.L., Pessenda, L.C.R., França, M.C., Magalhães, E., Yao, Q., 2022. Poleward mangrove expansion in South America coincides with MCA and CWP: a diatom, pollen, and organic geochemistry study. Quat. Sci. Rev. 288, 107598.

Ross, M.S., Ruiz, P.L., Sah, J.P., Hanan, E.J., 2009. Chilling damage in a changing climate in coastal landscapes of the subtropical zone: a case study from south Florida. Glob. Chang. Biol. 15, 1817–1832.

Ryu, J., Liu, K.B., McCloskey, T.A., 2022. Temporal variability in the relative strength of external drivers controlling ecosystem succession in a coastal wetland near Bayou Lafourche, southeast Louisiana, USA. Quat. Sci. Rev. 276, 107292.

Saintilan, N., Khan, N.S., Ashe, E., Kelleway, J.J., Rogers, K., Woodroffe, C.D., Horton, B.P., 2020. Thresholds of mangrove survival under rapid sea level rise. Science 368 (6495), 1118–1121. https://doi.org/10.1126/science.aba2656.

Saunders, R., Russo, M., 2011. Coastal shell middens in Florida: a view from the Archaic period. Quat. Int. 239 (1–2), 38–50.

Sherrod, C.L., McMillan, C., 1985. The distributional history and ecology of mangrove vegetation along the northern Gulf of Mexico coastal region. Contrib. Mar. Sci. 28, 129–140.

Simard, M., Zhang, K., Rivera-Monroy, V.H., Ross, M.S., Ruiz, P.L., Castañeda-Moya, E., Twilley, R.R., Rodriguez, E., 2006. Mapping height and biomass of mangrove forests in Everglades National Park with SRTM elevation data. Photogramm. Eng. Remote Sens. 72 (3), 299–311.

Snyder, C.M., Feher, L.C., Osland, M.J., Miller, C.J., Hughes, A.R., Cummins, K.L., 2022. The distribution and structure of mangroves (Avicennia germinans and Rhizophora mangle) near a rapidly changing range limit in the northeastern Gulf of Mexico. Estuar. Coasts 45 (1), 181–195.

Stein, J.C., Yu, Y., Copetti, D., Zwickl, D.J., Zhang, L., Zhang, C., Chougule, K., Gao, D., Iwata, A., Goicoechea, J.L., Wei, S., 2018. Genomes of 13 domesticated and wild rice relatives highlight genetic conservation, turnover and innovation across the genus Oryza. Nat. Genet. 50 (2), 285–296.

Stevens, P.W., Fox, S.L., Montague, C.L., 2006. The interplay between mangroves and saltmarshes at the transition between temperate and subtropical climate in Florida. Wetl. Ecol. Manag. 14 (5), 435–444. https://doi.org/10.1007/s11273-006-0006-3.

Stuart, S.A., Choat, B., Martin, K.C., Holbrook, N.M., Ball, M.C., 2007. The role of freezing in setting the latitudinal limits of mangrove forests. New Phytol. 173 (3), 576–583. https://doi.org/10.1111/j.1469-8137.2006.01938.x.

Tallis, J.H., 1991. Plant Community History: Long-term Changes in Plant Distribution And Diversity (No. 581.38 T3). Chapman and Hall, London.

Tomlinson, P.B., 2016. The Botany of Mangroves. Cambridge University Press.

Toscano, M.A., Macintyre, I.G., 2003. Corrected western Atlantic Sea-level curve for the last 11,000 years based on calibrated 14C dates from Acropora palmata framework and intertidal mangrove peat. Coral Reefs 22 (3), 257–270.

Toscano, M.A., Macintyre, I.G., 2003. Corrected western Atlantic sea-level curve for the last 11,000 years based on calibrated 14C dates from Acropora palmata framework and intertidal mangrove peat. Coral Reefs 22, 257–270.

U.S Climate Data, https://www.usclimatedata.com/climate/chiefland/florida/united-states/usfl0598 accessed May 2022.

Urrego, L.E., Bernal, G., Polanía, J., 2009. Comparison of pollen distribution patterns in surface sediments of a Colombian Caribbean mangrove with geomorphology and vegetation. Rev. Palaeobot. Palynol. 156 (3–4), 358–375.

Urrego, L.E., González, C., Urán, G., Polanía, J., 2010. Modern pollen rain in mangroves from San Andres Island, Colombian Caribbean. Rev. Palaeobot. Palynol. 162 (2), 168–182.

van Soelen, E.E., Brooks, G.R., Larson, R.A., Damsté, J.S.S., Reichart, G.J., 2012. Mid- to late-Holocene coastal environmental changes in southwest Florida, USA. The Holocene 22, 1–10.

Vogt, J., Skóra, A., Feller, I.C., Piou, C., Coldren, G., Berger, U., 2012. Investigating the role of impoundment and forest structure on the resistance and resilience of mangrove forests to hurricanes. Aquat. Bot. 97, 24–29. https://doi.org/10.1016/J.AQUABOT.2011.10.006.

Walker, W.H., Meléndez-Fernández, O.H., Nelson, R.J., Reiter, R.J., 2019. Global climate change and invariable photoperiods: a mismatch that jeopardizes animal fitness. Ecol. Evol. 9 (17), 10044–10054. https://doi.org/10.1002/ece3.5537.

Wallis, N.J., 2008. Networks of history and memory: creating a nexus of social identities in Woodland period mounds on the lower St. Johns River,Florida. J. Soc. Archaeol. 8 (2), 236–271.

Wallis, N.J., McFadden, P.S., 2019. A woodland period environmental and settlement history of Horseshoe Cove, northern Gulf Coast of Florida. Florida Anthropol. 71 (3–4), 191–206.

Wanless, H.R., Parkinson, R.W., Tedesco, L.P., 1994. Sea level control on stability of Everglades wetlands. In: Davis, S.M., Ogden, J.C. (Eds.), Everglades, the Ecosystem And Its Restoration. St. Lucie Press, p. 199 ± 222.

Ward, R.D., Friess, D.A., Day, R.H., Mackenzie, R.A., 2016. Impacts of climate change on mangrove ecosystems: a region by region overview. Ecosyst.HealthSustain. 2 (4). https://doi.org/10.1002/ehs2.1211.

Wentworth, C.K., 1922. A scale of grade and class terms for clastic sediments. J.Geol. 30 (5), 377–392.

Willard, D.A., Cooper, S.R., Gamez, D., Jensen, J., 2004. Atlas of pollen and spores of the Florida Everglades. Palynology 28 (1), 175 ± 227.

Williams, H.F., Beaubouef, C.E., Liu, K.B., Culligan, N., Riedlinger, L., 2022. Testing XRF identification of marine washover sediment beds in a coastal lake in southeastern Texas, USA. Mar. Geol. 443, 106705.

Woodroffe, C.D., Grindrod, J., 1991. Mangrove biogeography: the role of quaternary environmental and sea-level change. J. Biogeogr. 18, 479–492.

Yao, Q., Liu, K.B., 2017. Dynamics of marsh-mangrove ecotone since the mid-Holocene: a palynological study of mangrove encroachment and sea level rise in the Shark River Estuary, Florida. PloS one 12 (3), e0173670. https://doi.org/10.1371/journal.pone.0173670.

Yao, Q., Liu, K.B., 2018. Changes in modern pollen assemblages and soil geochemistry along coastal environmental gradients in the Everglades of south Florida. Front. Ecol. Evol. 5, 178.

Yao, Q., Liu, K.B., Platt, W.J., Rivera-Monroy, V.H., 2015. Palynological reconstruction of environmental changes in coastal wetlands of the Florida Everglades since the mid-Holocene. Quat. Res. 83 (3), 449–458. https://doi.org/10.1016/j.yqres.2015.03.005.

Yao, Q., Liu, K.B., Williams, H., Joshi, S., Bianchette, T.A., Ryu, J., Dietz, M., 2020a. Hurricane Harvey storm sedimentation in the San Bernard national wildlife refuge, Texas: fluvial versus storm surge deposition. Estuar. Coasts 43 (5), 971–983.

Yao, Q., Liu, K.B., Aragón-Moreno, A.A., Rodrigues, E., Xu, Y.J., Lam, N.S., 2020. A 5200-year paleoecological and geochemical record of coastal environmental changes and shoreline fluctuations in southwestern Louisiana: implications for coastal sustainability. Geomorphology 365, 107284.

Yao, Q., Liu, K.B., Wu, Y., Aragón-Moreno, A.A., Rodrigues, E., Cohen, M., de Souza, A.V., Farfán, L.M., Antinao, J.L., 2021. A multi-proxy record of hurricanes, tsunami, and post-disturbance ecosystem changes from coastal southern Baja California. Sci. Total Environ. 796, 149011.

Yao, Q., Rodrigues, E., Liu, K.B., Snyder, C., Culligan, N., 2022a. A Late-Holocene palynological record of coastal ecological change and climate variability from Apalachicola, Florida, U.S.A. Clim. Chang. Ecol. https://doi.org/10.1016/j.ecochg.2022.100056.

Yao, Q., Cohen, M.C.L., Liu, K.B., Fan, D., Rodrigues, E., Maiti, K., de Souza, A.V., Aragón-Moreno, A.A., Rohli, R., Yin, D., Pessenda, L.C.R., 2022b. Mangrove expansion at poleward range limits in North and South America: Late-Holocene climate variability or anthropocene global warming? Catena 216, 106413.

Yao, Q., Cohen, M.C.L., Liu, K.B., de Souza, A.V., Rodrigues, E., 2022c. Nature versus humans in coastal environmental change: assessing the impacts of Hurricanes Zeta and Ida in the context of beach nourishment projects in the Mississippi River Delta. Remote Sens. 14, 2598. https://doi.org/10.3390/rs14112598.

Yao, Q., Liu, K.B., Rodrigues, E., 2022d. Pre–treatment method to avoid contamination for radiocarbon dating of organic–rich coastal deposits. MethodsX 9, 101745. https://doi.org/10.1016/j.scitotenv.2021.149011.

You, A.Z., 2008. Comparative study of chemical composition of sediments from different water systems and estuaries of Fujian province. Geophys.Geochem.Explor. 32, 28–30.

Zhang, Z., Yao, Q., Liu, K.B., Li, L., Yin, R., Wang, G., Sun, J., 2021. Historical flooding regime along the Amur River and its links to East Asia summer monsoon circulation. Geomorphology 388, 107782.

Zhao, X., Liu, Y., Thomas, I., Salem, A., Wang, Y., Alassal, S.E., Jiang, F., Sun, Q., Chen, J., Finlayson, B., Wilson, P., 2022. Herding then farming in the Nile Delta. Commun. EarthEnviron. 3 (1), 1–7.

Zimmer, M., 2022. Mangrove forests: structure, diversity, ecosystem processes and threats. Encycl. Inl. Waters. 116–127. https://doi.org/10.1016/B978-0-12-819166-8.00149-3.